



Glacial cold-water coral growth in the Gulf of Cádiz: Implications of increased palaeo-productivity

Claudia Wienberg^{a,*}, Norbert Frank^b, Kenneth N. Mertens^c, Jan-Berend Stuur^{d,a}, Margarita Marchant^e, Jan Fietzke^f, Furu Mienis^{a,d}, Dierk Hebbeln^a

^a Center for Marine Environmental Sciences (MARUM), University of Bremen, Leobener Str., 28359 Bremen, Germany

^b Laboratoire des Sciences du Climat et de l'Environnement (LSCE), Bât.12, Avenue de la Terrasse, F-91198 Gif-sur-Yvette, France

^c Research Unit Palaeontology (RUP), Ghent University, Krijgslaan 281 S8, 9000 Ghent, Belgium

^d Royal Netherlands Institute for Sea Research (NIOZ), Landsdiep 4, 1797 SZ t'Horntje (Texel), The Netherlands

^e Departamento de Zoología, Facultad de Ciencias Naturales y Oceanográficas, Universidad de Concepción, Casilla 160-C, Concepción, Chile

^f Leibniz-Institute of Marine Sciences, IFM-GEOMAR, Wischhofstr. 1–3, 24148 Kiel, Germany

ARTICLE INFO

Article history:

Received 30 April 2010

Received in revised form 6 August 2010

Accepted 13 August 2010

Available online 15 September 2010

Editor: M.L. Delaney

Keywords:

cold-water corals
last glacial
productivity
aeolian dust
Gulf of Cádiz
NE Atlantic

ABSTRACT

A set of 40 Uranium-series datings obtained on the reef-forming scleractinian cold-water corals *Lophelia pertusa* and *Madrepora oculata* revealed that during the past 400 kyr their occurrence in the Gulf of Cádiz (GoC) was almost exclusively restricted to glacial periods. This result strengthens the outcomes of former studies that coral growth in the temperate NE Atlantic encompassing the French, Iberian and Moroccan margins dominated during glacial periods, whereas in the higher latitudes (Irish and Norwegian margins) extended coral growth prevailed during interglacial periods. Thus it appears that the biogeographical limits for sustained cold-water coral growth along the NE Atlantic margin are strongly related to climate change. By focussing on the last glacial–interglacial cycle, this study shows that palaeo-productivity was increased during the last glacial. This was likely driven by the fertilisation effect of an increased input of aeolian dust and locally intensified upwelling. After the Younger Dryas cold event, the input of aeolian dust and productivity significantly decreased concurrent with an increase in water temperatures in the GoC. This primarily resulted in reduced food availability and caused a widespread demise of the formerly thriving coral ecosystems. Moreover, these climate induced changes most likely caused a latitudinal shift of areas with optimum coral growth conditions towards the northern NE Atlantic where more suitable environmental conditions established with the onset of the Holocene.

© 2010 Elsevier B.V. All rights reserved.

1. Introduction

Along the NE Atlantic margin cold-water corals occur in a belt that extends from northern Norway (Barents Sea, 70°N; Lindberg et al., 2007) down to NW Africa (off Mauritania, 16°N; Colman et al., 2005). These ecosystems vary strongly with respect to their appearance, structure and coral vitality. Large flourishing *Lophelia*-reefs occur along the Norwegian margin. With a horizontal dimension of several hundred meters to kilometres they developed to the largest known living cold-water coral reefs worldwide (Fossà et al., 2005). Along the Irish margin cold-water corals are associated with coral mounds that vary in height from a few metres up to >380 m being often densely covered by living coral colonies (Wheeler et al., 2007, and refs. therein). Further to the south, cold-water corals mainly occur as isolated colonies or accumulations of fossil corals in the Bay of Biscay (Reveillaud et al., 2008), on seamounts (Duineveld et al., 2004) and

within canyons along the Iberian margin (Tyler et al., 2009), and on coral mounds along the NW African margin (Wienberg et al., 2009).

Along with the geographic distribution, a distinct stratigraphic pattern regarding the development of cold-water coral ecosystems along the NE Atlantic margin has been observed during the last glacial–interglacial cycle. Reefs of Holocene age on the Norwegian shelf started to develop after the retreat of glaciers at the termination of the last glacial (Freiwald et al., 2004). The Irish coral mounds seem to be restricted to interglacials with a very few exceptions (Dorschel et al., 2005; Eisele et al., 2008) and the latest re-establishment of cold-water coral ecosystems appears to have been started after the Younger Dryas (YD) cold reversal (Frank et al., 2009). To the south along the French, Iberian and Moroccan margins, corals are suggested to have been widely distributed during the last glacial (Schröder-Ritzrau et al., 2005; Wienberg et al., 2009). In actual fact, although the Gulf of Cádiz (GoC) was recently identified to be an important cold-water coral site in the temperate NE Atlantic, this area is at present mainly characterised by so-called 'coral graveyards' with only very few living corals (Foubert et al., 2008; Wienberg et al., 2009). Such current depauperation of live coral ecosystems might be explained by the recent warm and oligotrophic

* Corresponding author. Tel.: +49 421 21865652; fax: +49 421 2189865652.
E-mail address: cwberg@marum.de (C. Wienberg).

conditions in the GoC forcing reduced food availability (Wienberg et al., 2009). In addition, tidal currents and internal waves that have been identified to be important hydrodynamic processes for supplying food particles to and through the coral thickets (White et al., 2005, 2007) nowadays do not seem to play a major role in the GoC (Wienberg et al., 2009). However, the widespread occurrence of fossil corals suggests more favourable oceanographic conditions in the past. Indeed, initial datings revealed that cold-water corals have been common in the GoC during the last glacial (Wienberg et al., 2009).

The present study aims to refine and extend this observed stratigraphic pattern of coral occurrence along the NE Atlantic margin by 40 Uranium-series datings of reef-forming scleractinian cold-water corals from sediment cores retrieved in various areas of the GoC. Moreover, it is intended to relate the prosperity and/or demise of cold-water corals in the GoC to a distinct environmental and oceanographic setting that altered along with climate change. Thus, we aim to identify the main forcing factors triggering the development of cold-water coral ecosystems in the GoC.

2. Regional setting

The GoC is situated west of the Strait of Gibraltar, and thus connects the open North Atlantic Ocean and the Mediterranean Sea (Fig. 1). It is bordered by the Iberian Peninsula and the NW African coasts and extends from Cape St. Vincent at the southwestern tip of Portugal down to the Moroccan Atlantic margin at 33°N (Mauritzen et al., 2001). The Iberian continental shelf widens from ~15 km west of Faro to ~50 km further to the east (García-Lafuente and Ruiz, 2007), which is similar to the width of the Moroccan shelf (<60 km; Mittelstaedt, 1991).

The deeper basin of the GoC is characterised by a widespread occurrence of diapiric ridges and mud volcanoes (Somoza et al., 2003). Many of these mud volcanoes were identified to be covered by fossil cold-water corals (Somoza et al., 2003; Wienberg et al., 2009). Further conspicuous topographic features in the GoC are hundreds of coral mounds that are 20–30 m in height, and 50–200 m in length, and that are covered by fossil corals. They are restricted to the Moroccan

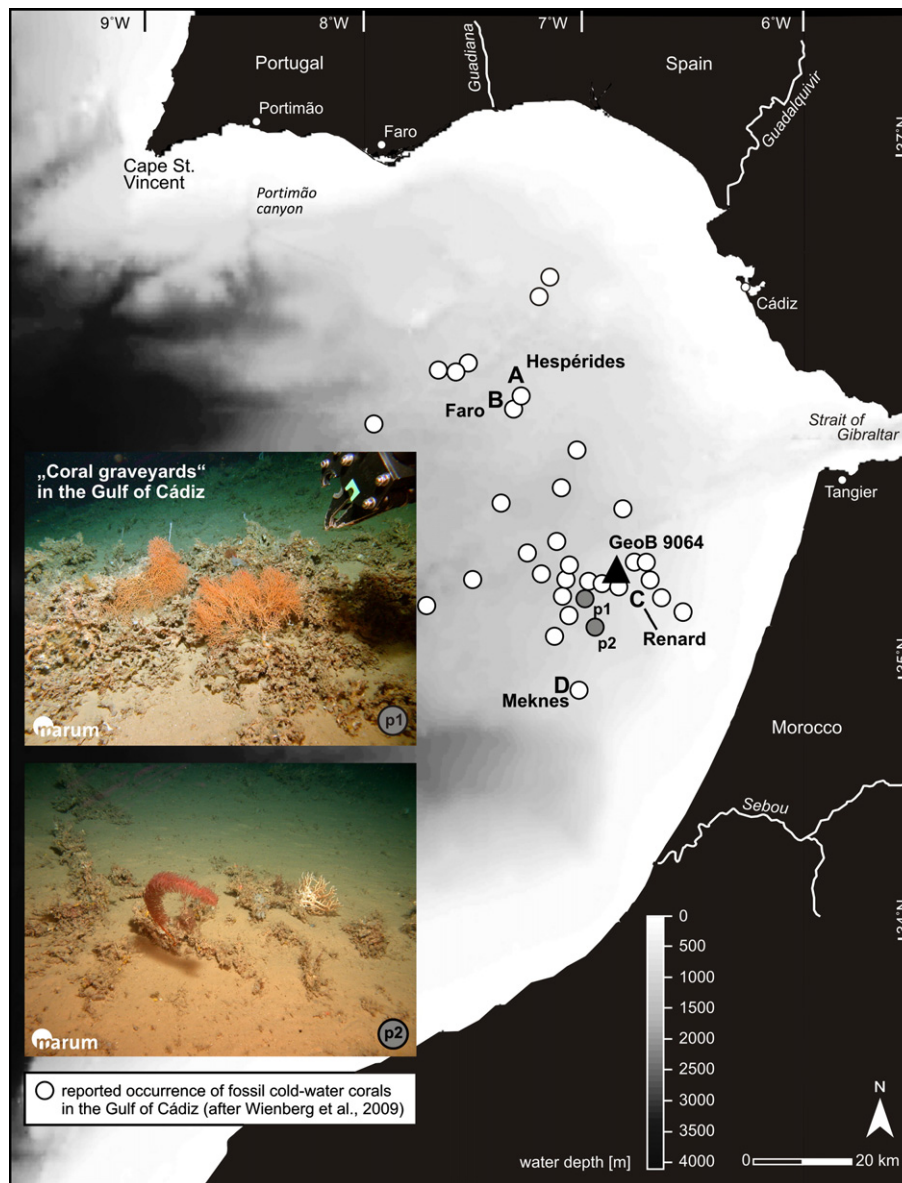


Fig. 1. Map of the Gulf of Cádiz (GoC) showing the coring sites (bathymetric data source: GEBCO). Reference sediment core GeoB 9064 (black triangle) and coral-bearing sediment cores (A–D). A: Hespérides mud volcano (GeoB 9018), B: Faro mud volcano (GeoB 9031, GeoB 9032), C: Renard Ridge (GeoB 9070, GeoB 12101, GeoB 12102, GeoB 12103, GeoB 12104, M2004-02), D: north of Meknes mud volcano (GeoB 12106). Indicated are the reported occurrences of fossil cold-water corals (after Wienberg et al., 2009). Lower left: photographs showing characteristic 'coral graveyards' in the southern GoC, Moroccan margin (position is indicated on the map as p1, p2) (images ©MARUM, Bremen).

margin where they have been found in a water depth between 400 and 960 m (Foubert et al., 2008; Hebbeln et al., 2008; Wienberg et al., 2009). The coral mounds are mainly arranged as clusters and are situated amidst mud volcanoes and on top of diapiric ridges. Detailed knowledge about their origin, composition, and temporal development is to date still lacking.

Present-day oceanographic circulation in the GoC is dominated by the exchange of water masses between the Atlantic Ocean and the Mediterranean Sea (Ochoa and Bray, 1991). The relatively cold Atlantic Inflow Water flows eastward along the Iberian margin partly entering the Mediterranean Sea. It is composed of North Atlantic Surficial Water and North Atlantic Central Water (NACW). The upper-thermocline NACW deepens from about 300 m water depth close to the Strait of Gibraltar to about 600 m in the outer and southern parts of the gulf (Ochoa and Bray, 1991; Mauritzen et al., 2001). Below this level occurs Mediterranean Outflow Water (MOW). Flowing westwards through the Strait of Gibraltar, the MOW prevails in the northern gulf where it flows between ~500 and 1400 m water depth above the North Atlantic Deep Water (NADW) (Ambar et al., 1999; Baringer and Price, 1999) and acts as a strong contour current (García et al., 2009). It is characterised by a permanent salinity maximum of ~36–37 and temperatures of 10.5 to 12 °C (Fusco et al., 2008). For the southern GoC along the Moroccan Atlantic margin information about its hydrography is basically lacking (Machín et al., 2006). However, Pelegrí et al. (2005) suggests the presence of MOW at 800 m. This assumption is supported by the presence of an anticyclone or meddy close to the Moroccan shelf which implies at least some temporary southward transport of MOW along the Moroccan margin (Carton et al., 2002).

Today, the GoC constitutes an oligotrophic system with diminished primary production in the surface waters (Behrenfeld et al., 2005). Cold and productive upwelling is restricted to a narrow band along the Portuguese coast (García-Lafuente and Ruiz, 2007), and to the NW African margin south of 31°N (Cape Ghir) (Mittelstaedt, 1991; Pelegrí et al., 2005). Due to a prevailing anticyclonic circulation (Pelegrí et al., 2005), the basin of the GoC separates the Iberian upwelling from the upwelling off NW Africa (García-Lafuente and Ruiz, 2007).

3. Materials and methods

3.1. Core locations

During three expeditions between 2003 and 2006, a set of ten coral-bearing sediment cores was collected from various sites in the GoC (Table 1). The coring sites comprise two mud volcanoes (Hespérides and Faro) along the Spanish margin and coral mounds along the Moroccan margin which are situated on top of the

prominent Renard Ridge and its easternmost extension, the Pen Duick Escarpment. Finally, the southernmost core was collected north of Meknes mud volcano (Fig. 1).

The sediment cores have a length between 2.2 m and 8.6 m and are made up of abundant cold-water coral fragments embedded in a hemipelagic sediment matrix (Table 1). The sediment cores collected from mud volcanoes along the Spanish margin only contain cold-water corals in their upper parts, whereas the cores retrieved from coral mounds along the Moroccan margin are characterised by the occurrence of coral fragments throughout the sedimentary record.

To reconstruct oceanographic and environmental changes in the GoC during the last glacial–interglacial cycle and to compare this with the temporal distribution pattern of cold-water corals, sediment core GeoB 9064 (35°24.91'N, 06°50.72'W, 702 m water depth) was selected for a multiproxy study (Fig. 1). Core GeoB 9064 was collected along the Moroccan margin (RV *Sonne* cruise SO175) and has a total length of 5.4 m. Samples for the various analyses were taken in 5-cm-intervals.

3.2. U/Th age determination on coral fragments

Forty fragments of the reef-forming scleractinian coral species *Madrepora oculata* and *Lophelia pertusa* were sampled at different core depths from the sediment cores listed in Table 1. Uranium-series measurements were performed using multi-collector ICP and thermionization mass spectrometry at IFM-GEOMAR (Kiel, Germany; Fietzke et al., 2005) and at LSCE (Gif-sur-Yvette, France; Frank et al., 2004; Douville et al., 2010). Prior to analyses, samples were carefully cleaned to remove contaminants from the fossil skeleton surfaces according to procedures described by Fietzke et al. (2005) and Frank et al. (2004). Isotope concentrations and ratios as well as the absolute dates on the cold-water corals are provided in Table 2. Whole procedure blank values of this sample set were measured to be around 2 pg for thorium (Th) and between 4 and 8 pg for uranium (U). Both values are negligible compared to U- and Th-concentrations of the studied corals. The reproducibility of mass spectrometric measurements was tested using international U standard materials such as HU1 and NBL112, which provided identical values as the ones published by Fietzke et al. (2005) and Frank et al. (2004).

3.3. Analyses on core GeoB 9064

3.3.1. AMS radiocarbon dating

Accelerator mass spectrometry (AMS) dating was performed at the Leibniz Laboratory for Age Determinations and Isotope Research (University of Kiel, Germany; Nadeau et al., 1997) and at the Poznań Radiocarbon Laboratory (Poznań, Poland). AMS ¹⁴C dates were

Table 1

Metadata of coral-bearing sediment cores collected from various sites in the Gulf of Cádiz (indicated in Fig. 1 as A, B, C, D). Abbreviations: Lat, latitude; Lon, longitude; Wd, water depth; Rec, recovery; Mv, mud volcano; Cm, coral mound; SM, Spanish margin; MM, Moroccan margin; PDE, Pen Duick Escarpment; Mo, *Madrepora oculata*; Lp, *Lophelia pertusa*. Cruises: 1, RV *Sonne* cruise SO175; 2, RV *Maria S. Merian* MSM01-3; 3, RV *Pelagia* cruise 64PE229.

| | Cruise | Location | Core-ID | Lat (°N) | Lon (°W) | Wd (m) | Rec (cm) | Coral content |
|---|---------|-----------------------|------------|-----------|-----------|--------|------------------|---|
| A | Mv SM 1 | Hespérides Mv | GeoB 9018 | 36°10.98' | 07°18.37' | 702 | 347 | 0–5 cm: dendrophylliids, 5–347 cm: solely Mo; strongly altered fragments. |
| B | Mv SM 1 | Faro Mv (lower flank) | GeoB 9031 | 36°05.75' | 07°23.28' | 897 | 484 | 0–160 cm: Mo-dominated; strongly altered fragments. |
| | Mv SM 1 | Faro Mv (top) | GeoB 9032 | 36°05.55' | 07°23.57' | 843 | 220 | 0–60 cm: Mo-dominated, 60–220 cm: mud breccia. |
| C | Cm MM 1 | Western Renard Ridge | GeoB 9070 | 35°22.00' | 06°51.90' | 594 | 560 ^a | 0–560 cm: Mo and Lp. |
| | Cm MM 2 | Western Renard Ridge | GeoB 12104 | 35°21.99' | 06°51.90' | 590 | 523 | 0–523 cm: Mo and Lp |
| | Cm MM 2 | Renard Ridge | GeoB 12102 | 35°21.11' | 06°50.96' | 585 | 518 | 0–518 cm: Mo, Lp, and dendrophylliids. |
| | Cm MM 2 | Renard Ridge | GeoB 12103 | 35°21.18' | 06°50.90' | 591 | 568 | 0–568 cm: Mo and Lp. |
| | Cm MM 2 | PDE | GeoB 12101 | 35°18.88' | 06°48.08' | 545 | 468 | 0–468 cm: Mo, Lp, and dendrophylliids. |
| | Cm MM 3 | PDE | M2004-02 | 35°17.68' | 06°47.25' | 523 | 861 | 0–861 cm: Mo, Lp, and dendrophylliids. |
| D | Cm MM 2 | North of Meknes Mv | GeoB 12106 | 34°59.49' | 07°04.56' | 758 | 303 | 30–303 cm: Mo and Lp. |

^a The uppermost 40 cm of core GeoB 9070 were disturbed due to coring operation, thus the undisturbed core depth ranges from 40 to 600 cm.

Table 2
Ages, isotope concentrations and ratios (n.a., not available; n.d. not dateable).

| N° | Sample ID | Depth (cm) | Coral | Labcode | Age (ka) | ± (ka) | ²³⁸ U (ppm) | ± (ppm) | ²³² Th (ppb) | ± (ppb) | δ ²³⁴ U(M) (‰) | ± (‰) | δ ²³⁴ U(0) (‰) | ± (‰) |
|----|------------|------------|-------|----------|----------|--------|------------------------|---------|-------------------------|---------|---------------------------|-------|---------------------------|-------|
| 1 | 2 | 3 | 4 | 5 | 6 | 7 | 8 | 9 | 10 | 11 | 12 | 13 | 14 | 15 |
| 01 | GeoB 9018 | 3 | Mo | n.a. | 14.65 | 0.09 | 4.020 | 0.004 | 21.019 | 0.052 | 149.8 | 1.9 | 156.1 | 2.0 |
| 02 | GeoB 9018 | 123 | Mo | n.a. | 294.00 | 7.00 | 4.329 | 0.004 | 3.021 | 0.006 | 73.1 | 1.4 | 167.7 | 3.3 |
| 03 | GeoB 9018 | 272 | Mo | n.a. | 283.80 | 8.50 | 4.005 | 0.004 | 23.536 | 0.064 | 61.9 | 1.5 | 138.0 | 3.3 |
| 04 | GeoB 9031 | 10 | Mo | n.a. | 20.92 | 0.12 | 4.956 | 0.005 | 21.400 | 0.055 | 139.9 | 1.8 | 148.5 | 1.9 |
| 05 | GeoB 9031 | 93 | Mo | n.a. | 37.25 | 0.23 | 5.263 | 0.007 | 4.796 | 0.009 | 132.8 | 2.3 | 147.5 | 2.5 |
| 06 | GeoB 9031 | 150 | Mo | n.a. | 45.94 | 0.33 | 4.338 | 0.004 | 8.875 | 0.016 | 120.6 | 1.4 | 137.4 | 1.6 |
| 07 | GeoB 9032 | 20 | Mo | n.a. | 17.15 | 0.15 | 4.447 | 0.005 | 62.092 | 0.192 | 140.6 | 1.6 | 147.6 | 1.7 |
| 08 | GeoB 9032 | 47 | Mo | n.a. | 41.17 | 0.25 | 4.512 | 0.005 | 25.841 | 0.070 | 130.3 | 1.8 | 146.4 | 2.0 |
| 09 | GeoB 9070 | 47 | Lp | n.a. | 23.50 | 0.12 | 4.622 | 0.003 | 4.428 | 0.010 | 137.9 | 1.1 | 147.3 | 1.2 |
| 10 | GeoB 9070 | 298 | Mo | n.a. | 43.68 | 0.28 | 3.552 | 0.003 | 51.216 | 0.079 | 129.6 | 1.8 | 146.6 | 2.0 |
| 11 | GeoB 9070 | 520 | Mo | n.a. | 166.00 | 2.40 | 3.968 | 0.004 | 15.089 | 0.033 | 78.7 | 1.7 | 125.9 | 2.7 |
| 12 | GeoB 12101 | 57 | Mo | Gif-1525 | n.d. | | 3.085 | 0.004 | 0.351 | 0.002 | 59.5 | 3.2 | / | / |
| 13 | GeoB 12101 | 146 | Lp | Gif-1389 | n.d. | | 3.214 | 0.004 | 0.920 | 0.003 | 47.4 | 3.0 | / | / |
| 14 | GeoB 12101 | 451 | Mo | Gif-1527 | 430.76 | 56.55 | 2.589 | 0.002 | 8.092 | 0.026 | 48.9 | 3.3 | 165.2 | 3.3 |
| 15 | GeoB 12102 | 28 | Mo | Gif-1529 | 57.96 | 0.74 | 4.390 | 0.005 | 0.316 | 0.001 | 119.5 | 2.7 | 140.8 | 2.7 |
| 16 | GeoB 12102 | 166 | Lp | Gif-1528 | 118.16 | 1.10 | 4.220 | 0.003 | 1.075 | 0.003 | 103.0 | 1.9 | 143.8 | 1.9 |
| 17 | GeoB 12102 | 238 | Lp | Gif-1390 | 152.27 | 5.12 | 3.035 | 0.003 | 0.306 | 0.003 | 112.1 | 2.9 | 172.4 | 2.9 |
| 18 | GeoB 12102 | 376 | Mo | Gif-1388 | 151.56 | 3.37 | 3.614 | 0.003 | 0.491 | 0.002 | 90.7 | 3.0 | 139.2 | 3.0 |
| 19 | GeoB 12102 | 493 | Mo | Gif-1386 | 164.02 | 2.01 | 3.194 | 0.003 | 0.495 | 0.002 | 99.5 | 1.8 | 158.3 | 1.8 |
| 20 | GeoB 12103 | 34 | Lp | Gif-1530 | 22.88 | 0.38 | 3.881 | 0.004 | 0.636 | 0.003 | 131.0 | 2.0 | 139.8 | 2.0 |
| 21 | GeoB 12103 | 88 | Lp | Gif-1392 | 25.72 | 0.39 | 4.462 | 0.006 | 3.873 | 0.010 | 128.7 | 2.9 | 138.4 | 2.9 |
| 22 | GeoB 12103 | 200 | Mo | Gif-1531 | 29.98 | 1.26 | 3.610 | 0.004 | 2.644 | 0.011 | 129.4 | 3.3 | 140.9 | 3.3 |
| 23 | GeoB 12103 | 317 | Mo | Gif-1532 | 30.43 | 0.96 | 3.828 | 0.004 | 0.192 | 0.003 | 126.9 | 2.2 | 138.3 | 2.2 |
| 24 | GeoB 12103 | 444 | Mo | Gif-1533 | 49.85 | 0.80 | 3.693 | 0.005 | 19.205 | 0.071 | 121.1 | 2.4 | 139.4 | 2.4 |
| 25 | GeoB 12104 | 8 | Lp | Gif-1387 | 23.57 | 0.18 | 4.435 | 0.003 | 7.778 | 0.016 | 126.3 | 1.7 | 135.0 | 1.7 |
| 26 | GeoB 12104 | 373 | Lp | Gif-1534 | 311.20 | 15.74 | 3.658 | 0.003 | 2.161 | 0.012 | 69.8 | 2.2 | 168.3 | 2.2 |
| 27 | GeoB 12104 | 491 | Mo | Gif-1535 | 342.29 | 25.38 | 3.492 | 0.004 | 2.003 | 0.008 | 71.1 | 2.6 | 187.1 | 2.6 |
| 28 | GeoB 12106 | 117 | Mo | Gif-1391 | 295.86 | 23.27 | 3.421 | 0.004 | 3.421 | 0.004 | 65.9 | 2.8 | 152.0 | 2.8 |
| 29 | M2004-02 | 49 | Mo | Gif-1631 | 9.15 | 0.71 | 3.512 | 0.011 | 0.103 | 0.014 | 149.3 | 3.0 | 153.2 | 3.0 |
| 30 | M2004-02 | 85 | Lp | Gif-1632 | 19.36 | 0.54 | 3.943 | 0.007 | 0.625 | 0.008 | 138.8 | 2.5 | 146.6 | 2.5 |
| 31 | M2004-02 | 105 | Lp | Gif-1633 | 19.87 | 0.52 | 3.284 | 0.010 | 0.695 | 0.006 | 136.0 | 3.9 | 143.9 | 3.9 |
| 32 | M2004-02 | 141 | Lp | Gif-1634 | 21.37 | 0.42 | 3.862 | 0.007 | 4.666 | 0.013 | 136.5 | 2.3 | 145.0 | 2.3 |
| 33 | M2004-02 | 147 | Lp | Gif-1635 | 22.75 | 0.26 | 4.016 | 0.006 | 2.209 | 0.006 | 133.0 | 2.9 | 141.8 | 2.9 |
| 34 | M2004-02 | 176 | Lp | Gif-1636 | 24.03 | 0.26 | 3.921 | 0.008 | 11.534 | 0.031 | 131.4 | 3.3 | 140.6 | 3.3 |
| 35 | M2004-02 | 247 | Lp | Gif-1637 | 34.90 | 0.43 | 3.099 | 0.004 | 0.310 | 0.001 | 130.3 | 2.5 | 143.8 | 2.5 |
| 36 | M2004-02 | 273 | Mo | Gif-1638 | 36.27 | 0.43 | 3.804 | 0.008 | 3.049 | 0.008 | 124.5 | 1.6 | 138.0 | 1.6 |
| 37 | M2004-02 | 313 | Lp | Gif-1639 | 142.08 | 1.92 | 4.068 | 0.010 | 2.908 | 0.009 | 96.6 | 2.3 | 144.4 | 2.4 |
| 38 | M2004-02 | 343 | Lp | Gif-1640 | 175.01 | 2.79 | 3.846 | 0.005 | 14.820 | 0.026 | 85.3 | 2.5 | 139.9 | 2.5 |
| 39 | M2004-02 | 363 | Mo | Gif-1641 | 242.07 | 8.35 | 3.174 | 0.008 | 0.506 | 0.003 | 85.4 | 2.7 | 169.3 | 2.7 |
| 40 | M2004-02 | 403 | Lp | Gif-1642 | 262.80 | 7.46 | 3.126 | 0.007 | 3.116 | 0.007 | 74.2 | 2.9 | 155.9 | 2.9 |

Note: Column 1: Sample label. Column 2: Depth in core. Column 3: Reef-forming scleractinian cold-water coral species, Lp *Lophelia pertusa*, Mo *Madrepora oculata*. Column 4: Labcode (not available for datings conducted at IFM-GEOMAR, N° 1–11). Column 5: Calculated coral ages. Column 6: ²³⁸U concentration. Column 7: ²³²Th concentration. Column 8: Measured ²³⁴U/²³⁸U activity ratios (δ²³⁴U(M)) are presented as deviation permil (‰) from the equilibrium value. Column 9: Decay corrected ²³⁴U/²³⁸U activity ratios (δ²³⁴U(0)) are calculated from the given ages and with λ_{234U}: 2.8263 × 10⁻⁶ yr⁻¹. Note that ages are strictly reliable having values between 146.6‰ and 149.6‰ (modern seawater), reliable with values of 149 ± 10‰, unreliable with values > 149 ± 10‰ (see also Stirling et al., 1998; Robinson et al., 2004; Esat and Yokoyama, 2006).

determined on ~8 mg calcium carbonate of mixed planktonic foraminifera. All ages were corrected for ¹³C and a mean ocean reservoir age of 400 years (Bard, 1988). AMS ¹⁴C ages were converted to calendar years using the CALPAL 2007 Hulu software (Joeris and Weninger, 1998) and are reported as calendar years before present (ka; Table 3).

3.3.2. Stable oxygen isotopes

The stable oxygen isotope (δ¹⁸O) composition of the planktonic foraminifera *Neogloboquadrina pachyderma* (dex.) was measured with a Finnigan MAT 251 mass spectrometer (Isotope Laboratory of the Department of Geosciences, University of Bremen, Germany). The isotopic composition was measured on the CO₂ gas evolved by treatment with phosphoric acid at a constant temperature of 75 °C. A working standard (Burgbrohl CO₂ gas) was applied, which has been calibrated against PDB by using the NBS18, 19 and 20 standards. Consequently, all δ¹⁸O data presented here are given relative to the PDB standard. Analytical standard deviation was about ± 0.07‰.

3.3.3. Grain-size analysis and end-member modelling

Grain sizes were measured on bulk and terrigenous material using a Malvern Instruments Mastersizer 2000 (Hydraulic Research Laboratory, Borgerhout, Belgium), which determines particle grain sizes between 0.26 μm and 2 046 μm grouped into 66 size classes. The terrigenous sediment fraction was obtained by treating bulk sediment with H₂O₂ (30% at 85 °C) and HCl (10% at 100 °C) to remove organic carbon and calcium carbonate, respectively. The sediments contained negligible amounts of biogenic opal, and microscopic analyses revealed that the applied method successfully removed all biogenic constituents. Finally, the samples were suspended in demineralised water by stirring and ultrasonic dispersion before analysis.

The terrigenous fraction of deep-sea sediments in the ocean is considered a mixture of ice-rafted, aeolian, and fluvial transported sediments. End-member modelling allows the distinction between possible lithic subpopulations of the grain-size spectrum (Weltje, 1997) that can be assigned to different sediment transport mechanisms (e.g., Stuut et al., 2002; Holz et al., 2007). To estimate the minimum number of end-members (EM) required for a satisfactory approximation of the data, the coefficients of determination were

Table 3

AMS ^{14}C dates determined on multi-species samples of planktonic foraminifera from sediment core GeoB 9064. The AMS ^{14}C ages were corrected for ^{13}C and a mean ocean reservoir age of 400 years, and were converted to calendar years using the CALPAL 2007 Hulu software. Estimated sedimentation rates for core GeoB 9064 are supplemented.

| Core depth (cm) | Labcode | Conventional age | | CALPAL age | | Sedimentation rate (cm kyr $^{-1}$) |
|--------------------|-----------|---------------------|-------------|-------------------------------------|-------------|---|
| | | ^{14}C age | \pm error | 1 σ (68%) | \pm error | |
| | | (years) | | (calendar years B.P., P. = AD 1950) | | |
| 4 | Poz-20282 | 2095 | 30 | 1630 | 50 | – |
| 74 | KIA-10065 | 9665 | 60 | 10430 | 100 | 7.95 |
| 169 | KIA-13060 | 12660 | 80 | 14370 | 240 | 24.11 |
| 289 | KIA-23840 | 23440 | 180 | 27860 | 190 | 8.90 |
| 399 | KIA-29420 | 29020 | 320 | 33090 | 420 | 21.03 |
| 524 | KIA-35660 | 35260 | 630 | 39960 | 960 | 18.20 |

calculated. These coefficients represent the proportion of the variance of each grain-size class that can be reproduced by the approximated data. This proportion is equal to the squared correlation coefficient (r^2) of input variables and their approximated values (Weltje, 1997; Prins and Weltje, 1999). As the terrigenous sediment fraction from the southern GoC is relatively fine-grained ($<170\ \mu\text{m}$), the number of input variables for the end-member model of core GeoB 9064 was reduced from 66 to 47 classes in the range of 0.29–170 μm .

3.3.4. Planktonic foraminiferal assemblage

The analysis for planktonic foraminiferal relative abundance counts is based on the $>150\ \mu\text{m}$ fraction. For each sample a minimum of ~ 200 specimens were identified following the taxonomy of planktonic foraminifera proposed by Hemleben et al. (1989). For *N. pachyderma* the relative abundances of right (dex.) and left (sin.) coiling individuals were determined, and the two forms were treated as individual species. The data are represented as percentages of total planktonic foraminiferal number.

4. Results

4.1. U-series dating

All selected coral fragments indicated minor to moderate physico-chemical alteration or dissolution which may disturb U-series ages. Initial $\delta^{234}\text{U}_0$ values are variable and range between $125.9 \pm 2.7\%$ and $187.1 \pm 2.6\%$ (Table 2, Fig. 2). Measured ^{232}Th concentrations are small ($<10\ \text{ng g}^{-1}$) for 75% of all samples (Fig. 2) but clearly specimens of *M. oculata* reveal more residual Th than *L. pertusa* (Table 2). This is a consequence of the cleaning procedure as the thinner polyps and more fragile skeleton of *M. oculata* is by far more difficult to clean. However, Th contamination is negligible since in general the $^{230}\text{Th}/^{232}\text{Th}$ activity ratios are >1000 .

Calculated U-series ages from all investigated coral sites in the GoC range from 9.2 ka to more than 400 ka (Fig. 3). Two samples from core GeoB 12101 could not be dated due to above equilibrium radioactive isotopic composition indicating U-series open system behaviour. More than 90% of all obtained ages correspond to glacial periods (Marine Isotope Stage (MIS) 2 back to MIS12), and 70% of these glacial coral ages cluster within the last glacial (MIS2–4) (Fig. 3). With regard to the initial $\delta^{234}\text{U}_0$, it is evident that the scatter increases largely beyond a coral age of 150 ka which is clearly indicative of increasing U-series system opening (Thompson et al., 2003; Scholz et al., 2004; Frank et al., 2006; Robinson et al., 2006). Consequently, those ages are less precise than the measured uncertainty would suggest which has to be taken in consideration for our data interpretation. Coral ages between 14 and 60 ka yield a mean initial $\delta^{234}\text{U}_0$ of $143.2 \pm 2.3\%$ ($n = 22$, 2σ standard deviation), which is slightly lower than measured in modern corals and seawater (146.6–149.6%; Delanghe et al., 2002; Robinson et al., 2004). Thus either corals suffer from minor U-series system opening, and thus, preferential loss of ^{234}U , or the glacial mean value of seawater was slightly lower than compared to today as suggested by Esat et al. (1999). Overall we consider that within a range of $149 \pm 10\%$ calculated ages are representing the chronological ages of the corals within the uncertainty of measurement (see also Stirling et al., 1998; Robinson et al., 2004; Esat and Yokoyama, 2006). However, we are aware that a more detailed analysis of the U-series data and uncertainties considering potential seawater U-isotopic variations, diagenetic alteration and U-series system opening is needed to improve in particular the quality of coral ages beyond 150 ka.

4.2. Age model core GeoB 9064

The age model of core GeoB 9064 for the last ~ 40 kyr is based on six AMS ^{14}C age control points and linear interpolation between these dates (Table 3, Fig. 4). The age model is supported by the correlation of the $\delta^{18}\text{O}$ measurements of the record (showing heavy $\delta^{18}\text{O}$ values of

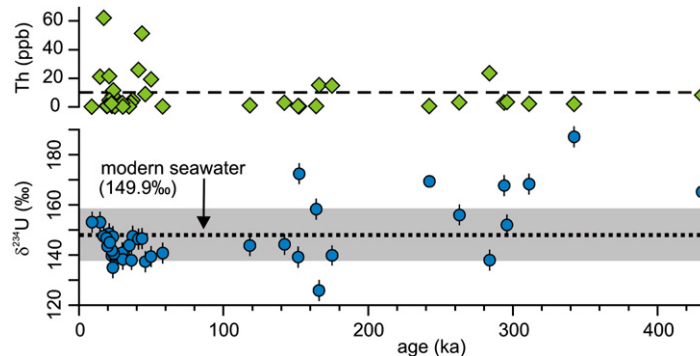


Fig. 2. Initial U-isotopic ratios of cold-water corals (lower graph) and ^{232}Th concentration (upper graph). $\delta^{234}\text{U}$ is in almost all cases very close to present-day seawater (149.9‰; black dotted line; range of $149.9 \pm 10\%$; light grey bar), except for the deepest sample in core GeoB 12104 (+38‰). ^{232}Th concentrations for 75% of all samples are below $10\ \text{ng g}^{-1}$ (black dashed line).

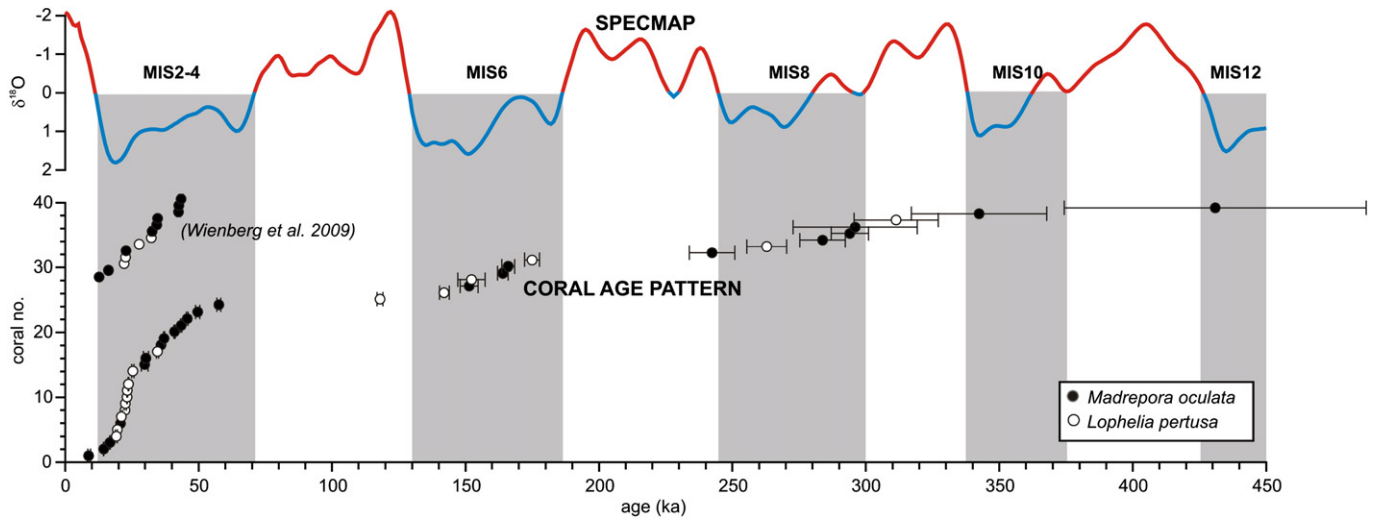


Fig. 3. $^{230}\text{Th}/\text{U}$ datings conducted on cold-water coral fragments collected in the GoC. AMS ^{14}C ages presented by Wienberg et al. (2009) are implemented. Note that solely reef-forming species such as *M. oculata* and *L. pertusa* are considered showing that >90% of all coral ages coincide with glacial periods. Marine Isotope Stages (MIS) are indicated by grey bars based on SPECMAP $\delta^{18}\text{O}$ stack (Imbrie et al. 1989).

1.5–2.5‰ for the last glacial and light values of <1.0‰ for the Holocene; Fig. 4) with the $\delta^{18}\text{O}$ record of the GRIP ice core (GRIP Members, 1993). The estimated average sedimentation rate is $\sim 16 \text{ cm ka}^{-1}$ (Table 3). Highest sedimentation rates of $18\text{--}24 \text{ cm ka}^{-1}$ occur during MIS3 and the last deglaciation. Lowest sedimentation rates of $8\text{--}9 \text{ cm ka}^{-1}$ are obtained for MIS2 and the Holocene (Fig. 4).

4.3. Grain size distribution and source

The median grain size of the terrigenous (bulk) fraction of sediment core GeoB 9064 varies between $5.71 \mu\text{m}$ ($5.93 \mu\text{m}$) and $12.03 \mu\text{m}$ ($17.88 \mu\text{m}$). The last glacial period and the Younger Dryas (YD) cold event are characterised by relatively coarse sediment deposition. In contrast, during the Holocene a distinct and continuous decrease of grain sizes is clearly visible ($6\text{--}9 \mu\text{m}$) (Fig. 4). A three-end-member model was created (with $r^2 = 0.77$) to describe the grain size data set of core GeoB 9064. The grain size distributions of the three end members are all unimodal, well-sorted and have relatively fine modal grain sizes with $25 \mu\text{m}$ for EM1, $16 \mu\text{m}$ for EM2, and $5 \mu\text{m}$ for EM3. Several sedimentological studies confirmed that aeolian sediments deposited in the deep-sea close to the continent are coarser grained than hemipelagic sediments with terrigenous sediments with mean grain sizes $>6 \mu\text{m}$ being generally attributed to aeolian transport, and sediments $<6 \mu\text{m}$ to hemipelagic transport (Ratmeyer et al., 1999; Prins et al., 2000). In addition, the mean modal sizes of present-day aeolian dust, collected along a transect of the NW African coast (33°N to 12°S) vary between $8 \mu\text{m}$ and $42 \mu\text{m}$ (Stuut et al., 2005). Hence, for core GeoB 9064, the two coarsest end members of the three-end-member model are considered to be of aeolian origin with EM1 interpreted as ‘coarse’ aeolian dust and EM2 as ‘fine’ aeolian dust. In contrast, EM3 is interpreted to result predominantly from fluvial input (Koopmann, 1981; Holz et al., 2007). During the last glacial, the aeolian content varies considerably between 30% and 60% and shows in particular during MIS3 rapid fluctuations. Close to the end of the last glacial ($\sim 17 \text{ ka}$), the aeolian content decreases before it increases again up to 60% during the YD. With the end of the YD ($\sim 11.5 \text{ ka}$), the proportion of the aeolian content on the total terrigenous fraction decreases continuously down to 25% (Fig. 4).

The EM1/EM2-ratio is considered as a measure for the relative wind intensity (Stuut et al., 2002). For core GeoB 9064, relatively high wind strength is indicated for the last glacial showing millennial-scale fluctuations. At $\sim 22 \text{ ka}$, the wind conditions changed dramatically. Within a time period of 1.5 kyr, wind intensity decreased remarkably

by 50% and stayed low during the entire Holocene (Fig. 4). This is deduced from a reduction of the content of ‘coarse’ aeolian dust (EM1) to almost zero, whereas the ‘fine’ aeolian dust (EM2) slightly increased towards the present.

4.4. Planktonic foraminiferal assemblage and abundance

The most abundant species in core GeoB 9064 is *N. pachyderma* dex. (27.1%), followed by *Globigerinita glutinata* (21.1%), *Globigerina bulloides* (15.8%), and *Globorotalia inflata* (12.2%). Together with *Globigerinoides ruber* (5.2%), *Globorotalia scitula* (4.5%), and *N. pachyderma* sin. (4.5%), these species account on average for >90% of the total planktonic foraminifera.

Maximum relative abundances of *N. pachyderma* dex. are recorded during the last glacial, contributing up to 60% of the total planktonic foraminifera fauna. At the end of the last glacial (15.5–14.5 ka), its relative abundances decreased remarkably down to 10%, followed by an increase up to 40% during the YD. At the end of the YD ($\sim 11.5 \text{ ka}$), relative abundances of *N. pachyderma* dex. significantly decreased down to <5% (Fig. 5). A similar trend is indicated for *N. pachyderma* sin., although it shows comparably lower abundances below 18%. Another abundant species during the last glacial was *G. glutinata* with relative abundances of 10–40%. During the course of the Holocene, its contribution was rather low with minimum rates of <10% except for the period between 10 and 8.5 ka, with relative abundances of up to 28%. An opposite trend to the above mentioned species is observed for *G. bulloides*. Relatively low abundance occurred during the last glacial (<20%), whereas during the Holocene, its relative contribution to the total fauna increased to >20%. In particular between 8.5 and 2 ka, *G. bulloides* was the most common species within the planktonic foraminiferal fauna with relative abundance of 30–48%. Between 40 and 18 ka, abundances of *G. inflata* were below 20%, and increased up to 38% until the onset of the YD. During the Holocene, its abundances varied between 8% and 20%. One distinct minimum (<10%) of *G. inflata* abundance is indicated between 10 and 8.5 ka that mirrors the concomitant maxima of *G. glutinata*. Contributions of *G. scitula* to the total fauna was rather moderate for most of the last glacial, and decreased remarkably around 18 ka to <5%, and remained low thereafter (Fig. 5). During the last glacial and until the end of the YD ($\sim 11.5 \text{ ka}$), *G. ruber* shows a low abundance of 0–10% that increased to 10–25% during the Holocene. *Globigerinoides sacculifer* was even absent during the last glacial. This species is exclusively found during the Holocene with relative abundances of up to 7.5% (Fig. 5).

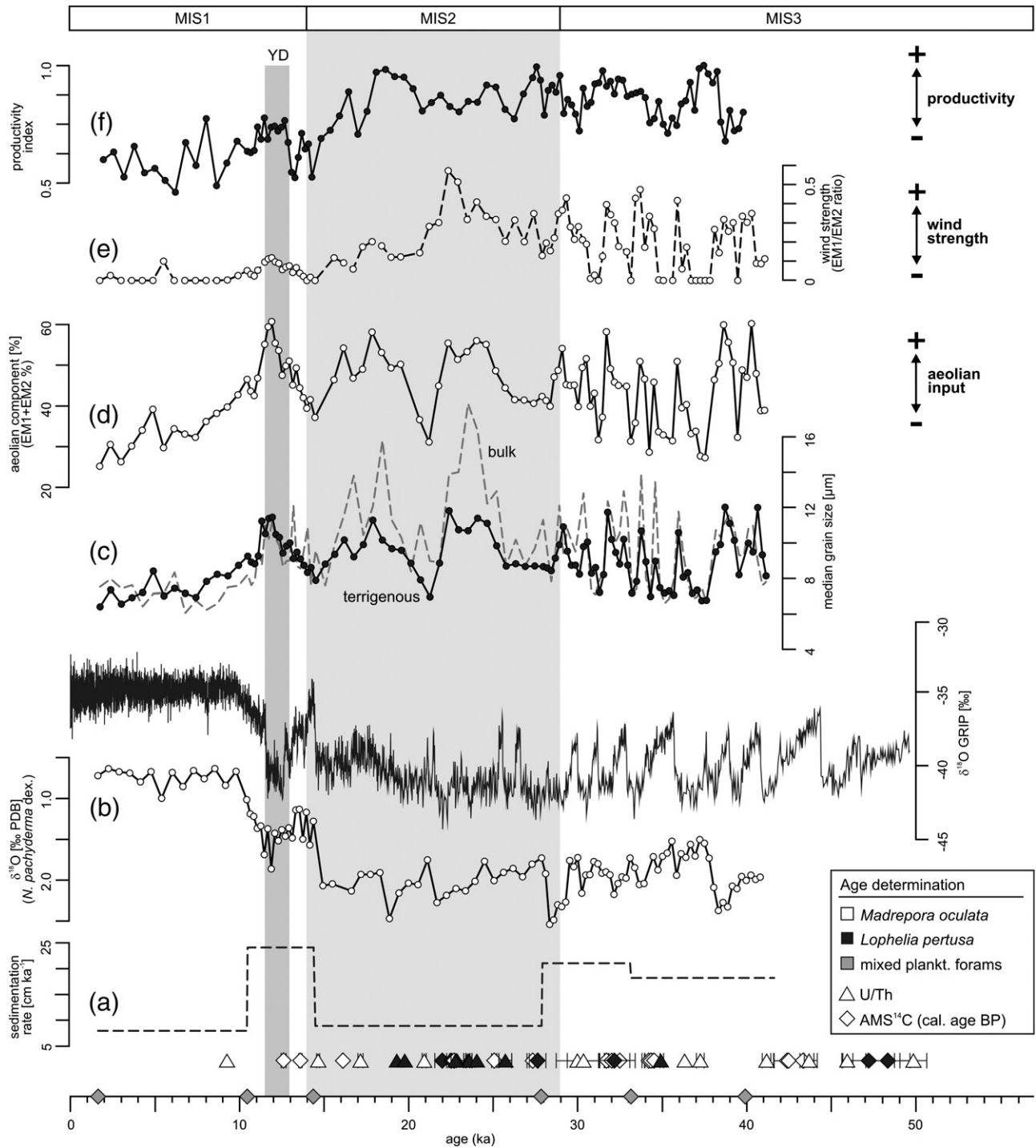


Fig. 4. Multi-proxy data of sediment core Geob 9064. (a) Estimated sedimentation rate, (b) stable oxygen isotopes record (lower curve) compared with the GRIP ice core record (upper curve) (c) median grain size (terrigenous and bulk sediment), (d) relative aeolian input, (e) relative wind strength, and (f) productivity index based on the ratio of high- to low-productivity planktonic foraminiferal assemblages. AMS ¹⁴C dates obtained for core Geob 9064 are marked by grey diamonds. For comparison, U/Th (squares; this study) and AMS ¹⁴C coral dates (triangles; Wienberg et al., 2009) obtained for the past 50 kyr are implemented. Note that solely reef-forming species such as *Madrepora oculata* and *Lophelia pertusa* are considered.

5. Discussion

5.1. Glacial coral growth phases in the Gulf of Cádiz

During the past years, much effort has been invested into dating cold-water corals from various sites along the NE Atlantic margin. The most comprehensive data set of coral ages exists for the Irish margin and reveals that coral growth in this area is restricted to the Holocene and prior interglacial periods (Frank et al., 2005; Rüggeberg et al., 2007; de Haas et

al., 2009; Frank et al., 2009). In contrast, for coral sites south of 50°N the data set of coral ages is rather scattered. However, the available dates suggest that the major phase of coral growth along the French, Iberian and Moroccan margins coincide with the last glacial period (Taviani et al., 1991; Schröder-Ritzrau et al., 2005; Wienberg et al., 2009).

For the GoC, it was shown that the reef-forming coral species *L. pertusa* and *M. oculata* have been restricted to a period between 12 and 45 ka (Wienberg et al., 2009). This preliminary result is confirmed by our data. In addition, the U/Th dates presented here show that

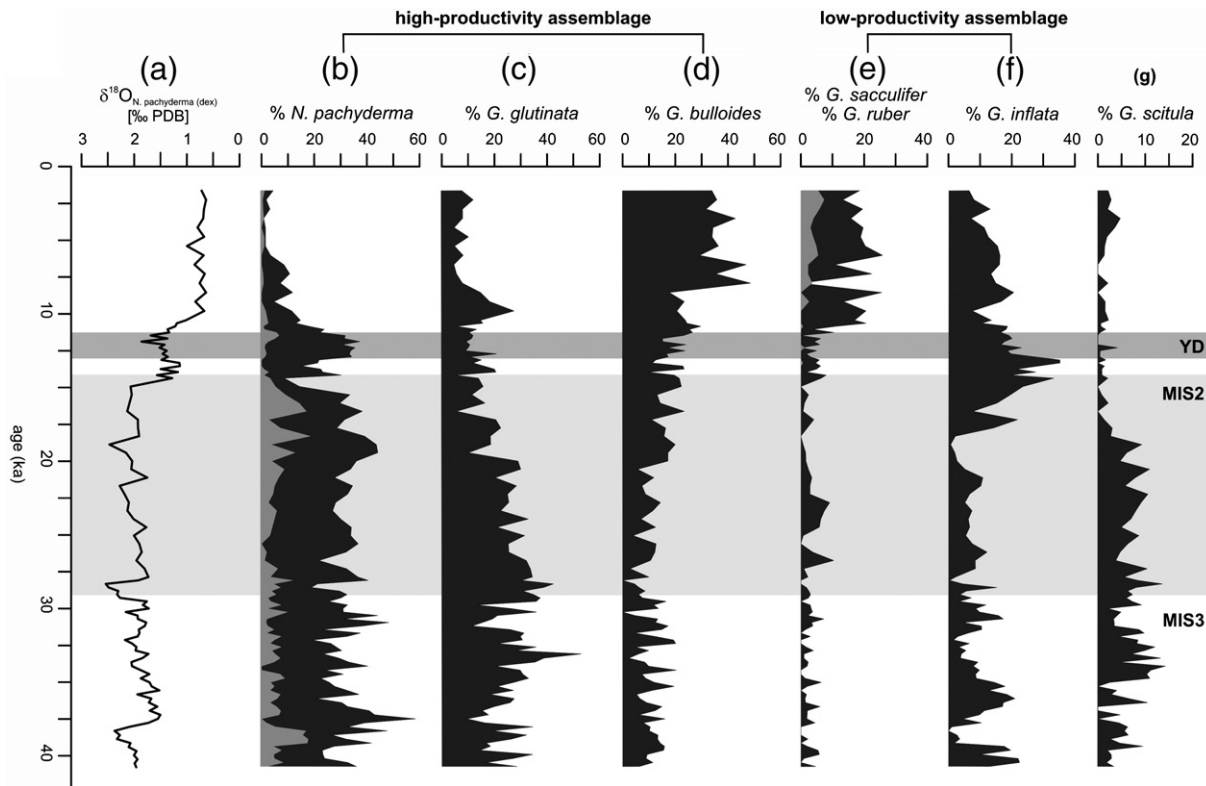


Fig. 5. The $\delta^{18}\text{O}$ record and planktonic foraminiferal abundance for sediment core GeoB 9064. (a) $\delta^{18}\text{O}_{\text{N. pachyderma (dex.)}}$ (‰ PDB), (b) *Neogloboquadrina pachyderma* (black: dex., grey: sin.), (c) *Globigerinita glutinata*, (d) *Globigerina bulloides*, (e) *Globigerinoides ruber* (black) and *Globigerinoides sacculifer* (grey), (f) *Globorotalia inflata*, (g) *Globorotalia scitula*. Younger Dryas (YD) and Marine Isotope Stages (MIS) 2 and 3 are indicated.

major phases of coral growth in the GoC are not solely restricted to the last glacial but also to prior glacial periods (back to MIS12), whereas during interglacials coral growth seems to be reduced or even absent (Fig. 2).

Most conspicuous is that the widespread decline of the coral ecosystems in the GoC during the YD cold reversal (12.9–11.5 ka) corresponds to the re-start of coral mound formation on Rockall Bank and the re-establishment of coral mound growth along the slopes of the Porcupine Seabight at around 11 ka (Frank et al., 2009). Regarding this pattern, we suggest that at the transition of the last glacial–interglacial, a latitudinal shift of areas with optimum cold-water coral growth conditions towards the northern NE Atlantic occurred that was most probably related to dramatic changes of the oceanographic and environmental conditions caused by climate change. Moreover, this northward shift happened rapidly over just a few hundreds of years and over a distance of 2000–2500 km (GoC to Irish margin).

Unfortunately, we still lack detailed understanding of the reproductive ecology and larval dispersal mode of scleractinian cold-water corals. Histological studies show that the cosmopolitan species *L. pertusa* exhibits an annual gametogenic cycle with spawning around January/February (Waller and Tyler, 2005). The widespread occurrence of *L. pertusa* and the rapid colonisation of man-made structures such as oil rigs (25 mm year⁻¹; Bell and Smith, 1999), point to a dispersive planula larva being capable to remain in the water column for several weeks.

5.2. Driving factors for coral growth

A combination of environmental and oceanographic conditions is required to promote a sustained development of cold-water coral ecosystems. Cold-water corals require (1) hard substrate to settle on, (2) protection against burial to grow, and (3) sufficient food supply. Therefore, they predominate in areas where strong currents prevail that reduce deposition of fine-grained sediments and supply large

quantities of food (Roberts et al., 2006). Today, thriving coral ecosystems occur in high concentrations in areas that are characterised by enhanced primary production in the surface waters of eutrophic systems, allowing a considerable part of the new production to be transported to the seafloor. In addition, tidal currents and internal waves have been identified (1) to enhance concentrations of organic matter at the shelf edge and (2) to transport fresh food particles to and through the cold-water coral reefs (Frederiksen et al., 1992; White et al., 2005, 2007). Recently, Dullo et al. (2008) indicated for the Celtic and Nordic margins that living cold-water corals occur within the density envelope of sigma-theta (σ_{θ}) = 27.35–27.65 kg m⁻³ emphasising the importance of physical boundary conditions. Finally, the world's most common cold-water coral species *L. pertusa* tend to be associated with oceanic water masses with a temperature of 4–12 °C (Roberts et al., 2006), and even up to 14 °C in the Mediterranean Sea (Taviani et al., 2005; Freiwald et al., 2009), salinities between 31.7 and 38.78 (Freiwald et al., 2004; Davies et al., 2008), and oxygen concentrations of 4.3–7.2 ml l⁻¹ (for the NE Atlantic; Davies et al., 2008).

For the GoC, all these requirements must have been fulfilled during glacial periods as cold-water corals were widespread during these times. During interglacial periods, these optimal environmental and oceanographic conditions must have been changed dramatically resulting in a widespread (gulf-wide) demise of the formerly thriving corals. As our obtained coral ages mainly cluster within the last glacial (~70%), the environmental and oceanographic changes of the GoC, focussing on the last glacial–interglacial cycle, are discussed in detail to identify the main forcing factors for coral growth in the GoC.

5.2.1. Effects of increased palaeo-productivity on cold-water coral growth

Strong vertical fluxes of labile organic matter, as often found in eutrophic regions, result in rich benthic fauna (e.g., De Stigter et al.,

1998; Schmiedl et al., 2000; Fontanier et al., 2002). In the NE Atlantic, seasonal algae blooms that sink rapidly to the deep-sea floor can even have a positive effect on the reproductive biology of benthic invertebrates (Billett et al., 1983; Thiel et al., 1989; Tyler et al., 1992), a relationship which is also hypothesised for *L. pertusa* and *M. oculata* thriving along the Irish margin (Waller and Tyler, 2005). Thus, enhanced productivity is a pre-requisite for a sustained development of healthy cold-water coral ecosystems. Indeed, regions with enhanced primary production as deduced from satellite-based observations of the chlorophyll content in surface waters (Behrenfeld et al., 2005) seem to mirror the recent distribution of thriving coral sites in the NE Atlantic.

Certain species of planktonic foraminifera strongly depend on primary productivity in the modern ocean (Hemleben et al., 1989), and hence downcore variations of the abundance of planktonic foraminiferal species within sedimentary records can be applied to assess palaeo-productivity conditions (e.g., Ivanova et al., 2003). In this context, the environmental constraints of the most abundant foraminiferal species identified for the GoC are reviewed in detail.

G. bulloides mainly thrives in the surface mixed layer above the thermocline and prefers relatively cold and nutrient-rich waters (e.g., Ganssen and Kroon, 2000; Chapman, 2010). Moreover, this species preferably occurs in areas along the Iberian and NW African margins that are characterised by pronounced seasonal upwelling, and thus, by high phytoplankton density and prey abundance (Salgueiro et al., 2008; Wilke et al., 2009). The opportunistic and cosmopolitan species *G. glutinata* is also strongly associated with the increase in productivity during spring bloom events in the North Atlantic (Chapman, 2010). However, the distribution of this species is found to be even more significantly associated with productivity than that of *G. bulloides*, which can be explained by its diet that preferentially consists of diatoms (Bé and Tolderlund, 1971; Hemleben et al., 1989; Schiebel et al., 2001). The sub-polar species *N. pachyderma* dex. prefers colder waters than *G. bulloides* (Bé and Tolderlund, 1971). Off the northern Iberian margin, high percentages of this species have been related to increased productivity generated by high river runoff (Salgueiro et al., 2008). In the GoC, *G. glutinata* and *N. pachyderma* dex. clearly dominate the foraminiferal assemblage during the last glacial with relative abundances of 55 to 75% (Fig. 5), thus pointing to rather nutrient-rich and cold conditions compared to the following Holocene when both species account for only ~10%. However, although *G. bulloides* is regarded as an indicator for nutrient enriched conditions it shows an opposite trend compared to the other two species.

G. inflata is considered a non-upwelling species and high relative abundances of this species in the North Atlantic coincide with oligotrophic waters (Pflaumann et al., 2003; Salgueiro et al., 2008). The two surface-dwelling species *G. ruber* and *Globigerinoides sacculifer* show a preference towards oligotrophic conditions as well (e.g., Ivanova et al., 2003; Mohtadi et al., 2007). These species prefer warm and well stratified surface waters (Duplessy et al., 1981; Stoll et al., 2007; Chapman, 2010). For the NE Atlantic, a significant increase in the relative abundances of *G. sacculifer* is observed when surface stratification is at a maximum and high sea surface temperatures prevail (Chapman, 2010). The significant increase of *G. ruber* and *G. sacculifer* after the YD cold event as found in our record (Fig. 5) thus indicates such warm and well stratified conditions in the GoC during the Holocene.

Taking all these findings for the NE Atlantic into account, *G. sacculifer*, *G. ruber* and *G. inflata* are inferred to represent a low-productivity assemblage, whereas *G. glutinata*, *G. bulloides* and *N. pachyderma* dex. are grouped as indicators for enhanced productivity. Similar to the approach of Stoll et al. (2007), we calculated the ratio of both assemblages and interpreted this ratio as an indicator of productivity (Fig. 4f), regardless of their affinity to upwelling processes. This ratio clearly shows that during the last glacial palaeo-productivity was overall enhanced in the GoC, which is in

particular expressed by high relative abundances of *G. glutinata* (Fig. 5). Following the end of the last glacial, this ratio significantly changed towards more oligotrophic conditions (Fig. 4).

5.2.2. Implications of frontal upwelling on glacial productivity in the GoC

This pattern of eutrophic conditions during the last glacial and oligotrophic conditions during the Holocene found for the GoC might be explained by a shift of the Azores Front (Rogerson et al., 2004). The Azores Front marks a zone of strong hydrographic transition associated with enhanced biological production caused by locally intense upwelling (Alves and DeVerdière, 1999). Today, the easternmost extension of the Azores Front is situated at 30°N off the Moroccan margin (Gould, 1985; Schiebel et al., 2002), and hence, does not penetrate into the GoC that extends from 37°N to 33°N (Fig. 1). But there is evidence that the Azores Front shifted northward and thus penetrated eastward into the GoC prior to 16 ka and during the YD (Rogerson et al., 2004). Rogerson et al. (2004) indicated this glacial shift of the Azores Front towards the GoC by high abundances of the planktonic foraminifer *G. scitula* in their records. This deep-dwelling species (100–700 m water depth) (Schiebel et al., 2002) is used as an indicator for cool surface waters and enhanced vertical mixing at temperate latitudes (e.g., Thunell and Reynolds, 1984; Perez-Folgado et al., 2003). Today *G. scitula* is found in high numbers in the Azores Front where upwelling causes high productivity (Schiebel et al., 2002), but it is almost absent in the GoC (Rogerson et al., 2004). The record of core GeoB 9064 shows that *G. scitula* is common prior to the Last Glacial Maximum (LGM), but is rare throughout the Holocene (Fig. 5) pointing to enhanced productivity during the last glacial caused by frontal upwelling.

5.2.3. Fertilisation effect of aeolian dust

Besides the effect of locally intensified upwelling that likely occurred in the GoC during the last glacial also the high input of aeolian dust might have significantly enhanced glacial productivity in the area. Grain size data from various sediment cores in the GoC, including our data (Fig. 4), show that during the last glacial mean grain sizes were rather coarse compared to the following Holocene (e.g., Rogerson et al., 2005; Voelker et al., 2006). Up to now, these grain size variations have been primarily attributed to changes in the strength of the prevailing bottom currents implying that bottom current strength was enhanced during the last glacial probably caused by a shift and intensification of the MOW's flow pathway (Schönfeld and Zahn, 2000; Rogerson et al., 2005; Voelker et al., 2006). Another common finding for the GoC is a rather low Holocene sedimentation rate (e.g., Rogerson et al., 2005; Voelker et al., 2006). Rogerson et al. (2005) estimated a Holocene accumulation rate that is only one fifth of that of the last glacial, and thus is in agreement with our estimated rates (Fig. 4). They assumed that this tremendous change in sedimentation rate was caused by a higher sediment supply prior to the last deglaciation but without indicating the major source of sediments supplied to the GoC.

However, this study shows that the variations in grain size and sedimentation rate as found for the GoC are rather the result of changes in the source of the terrigenous sediments and the amount of sediment input. Our grain size data clearly reveal that during the last glacial the deposition of aeolian transported sediments prevailed in the GoC (Fig. 4). During this time rather arid and cold conditions prevailed over the NW African continent (Gasse, 2000), and the intensity of the northern trade winds, which transport the aeolian dust, was enhanced especially from about 36°N to 24°N (Sarnthein et al., 1981; Hooghiemstra et al., 1987; Moreno et al., 2002). This is supported by our record showing that wind strength off Morocco (35°N) was significantly enhanced during the last glacial (Fig. 4). With the end of the YD, the proportion of the aeolian content on the total terrigenous fraction decreased continuously from 60 to 25% (Fig. 4), corresponding to the African humid period, which is known to be

characterised by a relatively humid and green Sahara with significantly lower amounts of aeolian dust being produced (e.g., deMenocal et al., 2000; Gasse, 2000). The African humid period terminated at 5.5 ka and the area of the Saharan desert returned to a state of hyperarid conditions (deMenocal et al., 2000). However, wind strength remained relatively low compared to the strong glacial trade winds (Hooghiemstra et al., 1987) and dust fluxes have been estimated to be today 2–4 times lower compared to the LGM (Grousset et al., 1998). Also our data show no significant increase of the input of aeolian dust in the GoC after 5.5 ka until today (Fig. 4).

The large input of aeolian dust during the last glacial coincides with a prosperous cold-water coral community in the GoC (Fig. 4). The link between dust input and coral prosperity was probably established by a simple fertilisation effect. During periods of enhanced Saharan dust input over the NE Atlantic, the supply of iron and manganese to the surface ocean is enhanced as well (de Jong et al., 2007) which promotes primary production in the surface waters (e.g., Boyd et al., 2000), and as a consequence, also might increase food availability for the bathyal cold-water corals.

5.2.4. Limitation of water temperatures on the prosperity of cold-water corals

The planktonic foraminiferal abundance data of core GeoB 9064 is consistent with the thermal history of the LGM and deglaciation. The general warming of the North Atlantic at the transition from the last glacial to the Holocene is reflected by a considerable increase in the abundance of *G. ruber* and *G. sacculifer* and a concurrent decrease in abundance of *N. pachyderma* dex., which is even more pronounced after the YD cold reversal (Fig. 5). This pattern is in agreement with other foraminiferal fauna records from the GoC (Sierro et al., 1999; Rogerson et al., 2004). The change from rather cool towards warm surface waters after the end of the YD was most likely accompanied by a change in subsurface temperatures in intermediate water depths, thus having an impact on the bathyal cold-water corals. Regarding the average temperatures of the intermediate water masses prevailing in the GoC (NACW: ~12 °C, Ait-Ameur and Goyet, 2006; MOW: 10.5–12 °C, Fusco et al., 2008), it becomes obvious that at least today water temperatures are at the very upper tolerance for reef-forming scleractinian cold-water corals such as *L. pertusa* (12 °C; Roberts et al., 2006). Moreover, dendrophylliid coral species that prefer rather warm conditions compared to *L. pertusa* seem to have been more common during the late Holocene (Wienberg et al., 2009).

6. Conclusion

This study clearly shows that the occurrence of cold-water corals in the GoC is dominant within the last glacial and prior glacial periods and that hardly any cold-water corals exist in this region during interglacials. Moreover, it could be identified that at the end of the YD cold event a shift from eutrophic to oligotrophic and warm conditions have been responsible for the demise of the formerly thriving coral ecosystems. The enhanced productivity conditions during the last glacial have been most probably caused by (1) an enhanced input of aeolian dust and (2) a shift of the Azores Fronts towards the GoC causing locally intense upwelling. Both factors supported enhanced primary productivity in the GoC, and thus resulted in enhanced food availability for the corals. By comparing our data set for the GoC with coral ages from the Norwegian and Irish margins that reveal a sustained prosperity of coral ecosystems right after the YD, it appears that a northward shift of areas with optimum cold-water coral growth conditions took place during the transition from the last glacial to the recent interglacial. The cold-water corals responded very rapidly to climate change over just a few hundreds of years, and it is most likely that in the course of global warming going along with dramatic changes in the environmental setting this northward trend will further continue.

Acknowledgements

The research leading to these results (U/Th and radiocarbon dates) has received funding from the European Community's Seventh Framework Programme (FP7/2007–2013) under the HERMIONE project, grant agreement no 226354. In addition, this work is part of CARBONATE (palaeo-environmental reconstructions), an ESF EURO-CORES integrated project as part of the EuroMARC project cluster funded by the DFG. K.N. Mertens is a Postdoctoral Researcher funded by the FWO. M. Marchant acknowledges the Dirección de Investigación and Departamento de Zoología at the University of Concepción (Chile) and the German Academic Exchange Service (DAAD). On-board assistance by ship and scientific team during cruises SO175 with RV *Sonne* (2003), 64PE229 with RV *Pelagia* (2004) and MSM01-3 with RV *Maria S. Merian* (2006) is acknowledged. O. Pfannkuche, J. Schönfeld and L. Maignien are kindly thanked for their great scientific support during cruise MSM01-3. We further acknowledge the support of the staff of the LSCE Gif-sur-Yvette (E. Douville, E. Sallé, C. Noury), the German Leibniz Laboratory for Age Determination and Isotope Research (University of Kiel, Germany), and the Poznan Radiocarbon Laboratory (Poznan, Poland) in U/Th and radiocarbon dating as well as the staff of the Ghent University (M. Verreth, A. Raes, F. Mostaert) in the sample preparation and grain size analysis. Finally, A. Eisenhauer, M. Mohtadi and two anonymous reviewers are kindly thanked for their helpful discussions and comments.

References

- Ait-Ameur, N., Goyet, C., 2006. Distribution and transport of natural and anthropogenic CO₂ in the Gulf of Cádiz. *Deep Sea Res. II* 53, 1329–1343.
- Alves, M., DeVerdière, A.C., 1999. Instability dynamics of a subtropical jet and applications to the Azores Front current system: eddydriven mean flow. *J. Phys. Oceanogr.* 29, 837–864.
- Ambar, I., Armi, L., Bower, A., Ferreira, T., 1999. Some aspects of time variability of the Mediterranean outflow. *Deep-Sea Res.* 26A, 1109–1136.
- Bard, E., 1988. Correction of accelerator mass spectrometry ¹⁴C ages measured in planktonic foraminifera: paleoceanographic implications. *Paleoceanography* 3, 635–645.
- Baringer, M.O., Price, J.F., 1999. A review of the physical oceanography of the Mediterranean outflow. *Mar. Geol.* 155, 63–82.
- Bé, A.W.H., Tolderlund, D.S., 1971. Distribution and ecology of living planktonic foraminifera in surface waters of the Atlantic and Indian Oceans. In: Funel, B.M., Riedel, W.R. (Eds.), *The Micropaleontology of Oceans*. Cambridge University Press, pp. 105–149.
- Behrenfeld, M.J., Boss, E., Siegel, D.A., Shea, D.M., 2005. Carbon-based ocean productivity and phytoplankton physiology from space. *Glob. Biogeochem. Cycles* 19, GB1006. doi:10.1029/2004GB002299.
- Bell, N., Smith, J.E., 1999. Coral growing on North Sea oil rigs. *Nature* 402, 601.
- Billett, D.S.M., Lampitt, R.S., Rice, A.L., Mantoura, R.F.C., 1983. Seasonal sedimentation of phytoplankton to the deep-sea benthos. *Nat. Geosci.* 302, 520–522.
- Boyd, P.W., Watson, A.J., Law, C.S., Abraham, E.R., Trull, T., Murdoch, R., Bakker, D.C.E., Bowie, A.R., Buesseler, K.O., Chang, H., Charette, M., Croot, P., Downing, K., Frew, R., Gall, M., Hadfield, M., Hall, J., Harvey, M., Jameson, G., LaRoche, J., Liddicoat, M., Ling, R., Maldonado, M.T., McKay, R., Nodder, S., Pickmere, S., Pridmore, R., Rintoul, S., Safi, K., Sutton, P., Strzepek, R., Tanneberger, K., Turner, S., Waite, A., Zeldis, J., 2000. A mesoscale phytoplankton bloom in the polar Southern Ocean waters stimulated by iron fertilization. *Nature* 407, 695–702.
- Carton, X., Chéribin, L., Paillet, J., Morel, Y., Serpette, A., Le Cann, B., 2002. Meddy coupling with a deep cyclone in the Gulf of Cádiz. *J. Mar. Syst.* 32, 13–42.
- Chapman, M.R., 2010. Seasonal production pattern of planktonic foraminifera in the NE Atlantic Ocean: implications for paleotemperature and hydrographic reconstructions. *Paleoceanography* 25, PA1101. doi:10.1029/2008PA001708.
- Colman, J.G., Gordon, D.M., Lane, A.P., Forde, M.J., Fitzpatrick, J., 2005. Carbonate mounds off Mauritania, Northwest Africa: status of deep-water corals and implications for management of fishing and oil exploration activities. In: Freiwald, A., Roberts, J.M. (Eds.), *Cold-water Corals and Ecosystems*. Springer, Heidelberg, pp. 417–441.
- Davies, A.J., Wisshak, M., Orr, J.C., Roberts, J.M., 2008. Predicting suitable habitat for the cold-water coral *Lophelia pertusa* (Scleractinia). *Deep Sea Res. I* 55, 1048–1062.
- de Haas, H., Mienis, F., Frank, N., Richter, T.O., Steinbacher, R., de Stigter, H., van der Land, C., van Weering, T.C.E., 2009. Morphology and sedimentology of (clustered) cold-water coral mounds at the south Rockall Trough margins, NE Atlantic Ocean. *Facies* 55, 1–26.
- de Jong, J.T.M., Boyé, M., Gelado-Caballero, M.D., Timmermans, K.R., Veldhuis, M.J.W., Nolting, R.F., van den Berg, C.M.G., de Baar, H.J.W., 2007. Inputs of iron, manganese and aluminium to surface waters of the Northeast Atlantic Ocean and the European continental shelf. *Mar. Chem.* 107, 120–142.

- De Stigter, H.C., Jorissen, F.J., Vand der Zwaan, G.J., 1998. Bathymetric distribution and microhabitat partitioning of live (Rose Bengal stained) benthic foraminifera along a shelf to deep sea transect in the southern Adriatic Sea. *J. Foramin. Res.* 28, 40–65.
- Delanghe, D., Bard, E., Hamelin, B., 2002. New TIMS constraints on the uranium-238 and uranium-234 in seawaters from the main ocean basins and the Mediterranean Sea. *Mar. Chem.* 80, 79–93.
- deMenocal, P., Ortiz, J., Guilderson, T., Adkins, J., Sarntheim, M., Baker, L., Yarusinsky, M., 2000. Abrupt onset and termination of the African Humid Period: rapid climate responses to gradual insolation forcing. *Quatern. Sci. Rev.* 19, 347–361.
- Dorschel, B., Hebbeln, D., Rüggeberg, A., Dullo, W.-C., 2005. Growth and erosion of a cold-water coral covered carbonate mound in the Northeast Atlantic during the Late Pleistocene and Holocene. *Earth Planet. Sci. Lett.* 233, 33–44.
- Douville, E., Sallé, E., Frank, N., Eisele, M., Pons-Branchu, E., Ayrault, S., 2010. Rapid and accurate Th–U dating of ancient carbonates using Inductively Coupled Plasma-Quadrupole Mass Spectrometry. *Chem. Geol.* 272, 1–11.
- Duineveld, G.C.A., Lavley, M.S.S., Berghuis, E.M., 2004. Particle flux and food supply to a seamount cold-water coral community (Galicia Bank, NW Spain). *Mar. Ecol. Prog. Ser.* 277, 13–23.
- Dullo, C., Flögel, S., Rüggeberg, A., 2008. Cold-water coral growth in relation to the hydrography of the Celtic and Nordic European continental margin. *Mar. Ecol. Prog. Ser.* 371, 165–176.
- Duplessy, J.C., Bé, A.W., Blanc, P.L., 1981. Oxygen and carbon isotopic composition and biogeographic distribution of planktonic foraminifera in the Indian Ocean. *Palaeogeogr. Palaeoclimatol. Palaeoecol.* 33, 9–46.
- Eisele, M., Hebbeln, D., Wienberg, C., 2008. Growth history of a cold-water coral covered carbonate mound – Galway Mound, Porcupine Seabight, NE-Atlantic. *Mar. Geol.* 253, 160–169.
- Esat, T.M., Yokoyama, Y., 2006. Variability in the uranium isotopic composition of the oceans over glacial–interglacial timescales. *Geochim. Cosmochim. Acta* 70, 4140–4150.
- Esat, T.M., McCulloch, M.T., Chappell, J., Pillans, B., Omura, A., 1999. Rapid fluctuations in sea level recorded at Huon Peninsula during the penultimate deglaciation. *Science* 283, 197–201.
- Fietzke, J., Liebetrau, V., Eisenhauer, A., Dullo, W.-C., 2005. Determination of uranium isotope ratios by multi-static MIC-ICP-MS: method and implementation for precise U- and Th-series isotopes. *J. Anal. At. Spectrom.* 20, 395–401.
- Fontanier, C., Jorissen, F.J., Licari, L., Alexandre, A., Anshutz, P., Carbonel, P., 2002. Live benthic foraminiferal faunas from the Bay of Biscay: faunal density, composition, and microhabitats. *Deep Sea Res.* 49, 751–785.
- Fosså, J.H., Lindberg, B., Christensen, O., Lundålv, T., Svellingen, I., Mortensen, P.B., Alsvag, J., 2005. Mapping of Lophelia reefs in Norway: experiences and survey methods. In: Freiwald, A., Roberts, J.M. (Eds.), *Cold-water Corals and Ecosystems*. Springer, Heidelberg, pp. 359–391.
- Foubert, A., Depreiter, D., Beck, T., Maignien, L., Pannemans, B., Frank, N., Blamart, D., Henriët, J.-P., 2008. Carbonate mounds in a mud volcano province off north-west Morocco: key to processes and controls. *Mar. Geol.* 248, 74–96.
- Frank, N., Paterne, M., Ayliffe, L., van Weering, T.C.E., Henriët, J.-P., Blamart, D., 2004. Eastern North Atlantic deep-sea corals: tracing upper intermediate water $\Delta^{14}\text{C}$ during the Holocene. *Earth Planet. Sci. Lett.* 219, 297–309.
- Frank, N., Lutringer, A., Paterne, M., Blamart, D., Henriët, J.-P., van Rooij, D., van Weering, T.C.E., 2005. Deep-water corals of the northeastern Atlantic margin: carbonate mound evolution and upper intermediate water ventilation during the Holocene. In: Freiwald, A., Roberts, J.M. (Eds.), *Cold-water Corals and Ecosystems*. Springer, Heidelberg, pp. 113–133.
- Frank, N., Turpin, L., Cabioch, G., Blamart, D., Tressens-Fedou, M., Colin, C., Jean-Baptiste, P., 2006. Open system U-series ages of corals from a subsiding reef in New Caledonia: implications for sea level changes, and subsidence rate. *Earth Planet. Sci. Lett.* 249, 274–289.
- Frank, N., Ricard, E., Lutringer-Paque, A., van der Land, C., Colin, C., Blamart, D., Foubert, A., Van Rooij, D., Henriët, J.-P., de Haas, H., van Weering, T.C.E., 2009. The Holocene occurrence of cold-water corals in the NE Atlantic: implications for coral carbonate mound evolution. *Mar. Geol.* 266, 129–142.
- Frederiksen, R., Jensen, A., Westerberg, H., 1992. The distribution of scleractinian coral *Lophelia pertusa* around the Faroe Islands and the relation to intertidal mixing. *Sarsia* 77, 157–171.
- Freiwald, A., Fosså, J.H., Grehan, A., Koslow, T., Roberts, J.M., 2004. Cold-water Coral Reefs. UNEP-WCMC, Biodiversity Series 22, Cambridge, UK, p. 84.
- Freiwald, A., Beuck, L., Rüggeberg, A., Taviani, M., Hebbeln, D., R/V Meteor Cruise M70-1 participants, 2009. The white coral community in the central Mediterranean Sea revealed by ROV surveys. *Oceanography* 22, 58–74.
- Fusco, G., Artale, V., Cotroneo, Y., Sannino, G., 2008. Thermohaline variability of Mediterranean Water in the Gulf of Cádiz, 1948–1999. *Deep Sea Res.* 55, 1624–1638.
- Ganssen, G., Kroon, D., 2000. The isotopic signature of planktonic foraminifera from the NE Atlantic surface sediments: implications for the reconstruction of past oceanic conditions. *J. Geol. Soc. Lond.* 157, 693–699.
- García, M., Hernández-Molina, F.J., Llave, E., Stow, D.A.V., León, R., Fernández-Puga, M.C., Diaz del Río, V., Somoza, L., 2009. Centourite erosive features caused by the Mediterranean outflow water in the Gulf of Cádiz: quaternary tectonics and oceanographic implications. *Mar. Geol.* 257, 24–40.
- García-Lafuente, J., Ruiz, J., 2007. The Gulf of Cádiz pelagic ecosystem: a review. *Oceanogr.* 74, 228–251.
- Gasse, F., 2000. Hydrological changes in the African tropics since the Last Glacial Maximum. *Quatern. Sci. Rev.* 19, 189–211.
- Gould, W.J., 1985. Physical oceanography of the Azores Front. *Prog. Oceanogr.* 14, 167–190.
- Grousset, F.E., Parra, M., Bory, A., Martinez, P., Bertrand, P., Shimmield, G., Ellam, R.M., 1998. Saharan wind regimes traced by the Sr–Nd isotopic composition of subtropical Atlantic sediments: Last Glacial Maximum vs. today. *Quatern. Sci. Rev.* 17, 395–409.
- Hebbeln, D., Wienberg, C., cruise participants, 2008. Report and preliminary results of RV Pelagia cruise 64PE284, Cold-water corals in the Gulf of Cádiz and on Coral Patch Seamount, Portimao – Portimao, 18.02.–09.03.2008: University of Bremen, Reports of the Department of Geosciences (GeoB) No. 265, p. 90.
- Hemleben, C., Spindler, M., Anderson, O.R., 1989. *Modern Planktonic Foraminifera*. Springer, New York, 363 pp.
- Holz, C., Stuet, J.B., Meggers, H., Rüdiger, H., 2007. Variability in terrigenous sedimentation processes off northwest Africa and its relation to climatic changes: inferences from grain-size distributions of a Holocene marine sediment record. *Sedimentol. Geol.* 202, 499–508.
- Hooghiemstra, H., Bechler, A., Beug, H.-J., 1987. Isopollen maps for 18,000 years BP of the Atlantic offshore of Northwest Africa: evidence for paleowind circulation. *Paleoceanography* 2, 561–582.
- Imbrie, J., Hays, J.D., Martinson, D.G., McIntyre, A., Mix, A.C., Morley, J.J., Pisias, N.G., Prell, W.L., Shackleton, N.J., 1989. The orbital theory of Pleistocene climate: support from a revised chronology of the marine $\delta^{18}\text{O}$ record. *Milankovitch and Climate: In: Berger, A. (Ed.), NATO ASI Series, Dordrecht*, pp. 269–305.
- Ivanova, E., Schiebel, R., Singh, A.D., Schmiedl, G., Niebler, H.-S., Hemleben, C., 2003. Primary production in the Arabian Sea during the last 135000 years. *Palaeogeogr. Palaeoclimatol. Palaeoecol.* 197, 61–82.
- Joeris, O., Weninger, B., 1998. Extension of the ^{14}C calibration curve to ca. 40,000 cal BC by synchronizing Greenland $^{18}\text{O}/^{16}\text{O}$ ice core records and North Atlantic foraminifera profiles: a comparison with U/Th coral data. *Radiocarbon* 40, 495–504.
- Koopmann, B., 1981. Sedimentation von Saharaarab auf subtropischen Nordatlantik während der letzten 25.000 Jahre. *Meteor. Forschungsergeb.* 35, 23–59.
- Lindberg, B., Berndt, C., Mienert, J., 2007. The Fugløy Reef at 70°N ; acoustic signature, geologic, geomorphologic and oceanographic setting. *Int. J. Earth Sci.* 96, 201–213.
- Machin, F., Pelegrí, J.L., Marrero-Díaz, A., Laiz, I., Ratsimandresy, A.W., 2006. Near-surface circulation in the southern Gulf of Cádiz. *Deep Sea Res.* 53, 1161–1181.
- Mauritzen, C., Morel, J., Paillet, J., 2001. On the influence of Mediterranean water on the central waters of the North Atlantic Ocean. *Deep-Sea Res.* 44, 1543–1574.
- Members, G.R.I.P., 1993. Climate instability during the last interglacial period recorded in the GRIP ice core. *Nature* 364, 203–207.
- Mittelstaedt, E., 1991. The ocean boundary along the northwest African coast: circulation and oceanographic properties at the sea surface. *Prog. Oceanogr.* 26, 307–355.
- Mohtadi, M., Max, L., Hebbeln, D., Baumgart, A., Krück, N., Jennerjahn, T., 2007. Modern environmental conditions recorded in surface sediment samples off W and SW Indonesia: planktonic foraminifera and biogenic compounds analyses. *Mar. Micropaleontol.* 65, 96–112.
- Moreno, A., Cacho, I., Canals, M., Prins, M.A., Sánchez-Goñi, M.-F., Grimalt, J.O., Weltje, G. J., 2002. Saharan dust transport and high-latitude glacial climatic variability: the Alboran Sea record. *Quatern. Res.* 58, 318–328.
- Nadeau, M.J., Schleicher, M., Grootes, P., Erlenkeuser, H., Gottolung, A., Mous, D.J.W., Sarntheim, M., Willkomm, N., 1997. The Leibniz-Labor AMS facility of the Christian-Albrechts University, Kiel, Germany. *Nucl. Instrum. Meth. Phys. Res.* 123, 22–30.
- Ochoa, J., Bray, N.A., 1991. Water mass exchange in the Gulf of Cádiz. *Deep-Sea Res.* 38 (S1), 5465–5503.
- Pelegrí, J.L., Marrero-Díaz, A., Ratsimandresy, A., Antoranz, A., Cisneros-Aguirre, J., Gordo, C., Grisolía, D., Hernández-Guerra, A., Láiz, I., Martínez, A., Parrilla, G., Pérez-Rodríguez, P., Rodríguez-Santana, A., Sangrà, P., 2005. Hydrographic cruises off northwest Africa: the Canary Current and the Cape Ghir region. *J. Mar. Syst.* 54, 39–63.
- Perez-Folgado, M., Sierro, F.J., Flores, J.A., Cacho, I., Grimalt, J.O., Zahn, R., Shackleton, N.J., 2003. Western Mediterranean planktonic foraminifera events and millennial climatic variability during the last 70 kyr. *Mar. Micropaleontol.* 48, 49–70.
- Pflaumann, U., Sarntheim, M., Chapman, M., d'Abreu, L., Funnel, B., Huels, M., Kiefer, T., Maslin, M., Schulz, H., Swallow, J., van Kreveld, S., Vautravers, M., Vogelsang, E., Weinelt, M., 2003. Glacial North Atlantic: sea-surface conditions reconstructed by GLAMAP 2000. *Paleoceanography* 18, 1065.
- Prins, M.A., Weltje, G.J., 1999. End-member modeling of siliciclastic grain-size distributions: the Late Quaternary record of eolian and fluvial sediment supply to the Arabian Sea and its paleoclimatic significance. In: Harbaugh, J., Watney, L., Rankey, G., Slingerland, R., Goldstein, R., Franseen, E. (Eds.), *Numerical Experiments in Stratigraphy: Recent Advances in Stratigraphic and Sedimentologic Computer Simulations*. SEPM, pp. 91–111.
- Prins, M.A., Postma, G., Cleveringa, J., Cramp, A., Kenyon, N.H., 2000. Controls on terrigenous sediment supply to the Arabian Sea during the late Quaternary: the Indus Fan. *Mar. Geol.* 169, 327–349.
- Ratmeyer, V., Balzer, W., Bergametti, G., Chiappello, I., Fischer, G., Wyputta, U., 1999. Seasonal impact of mineral dust on deep-ocean particle flux in the eastern subtropical Atlantic Ocean. *Mar. Geol.* 159, 241–252.
- Reveillaud, J., Freiwald, A., Van Rooij, D., Le Guilloux, E., Altuna, A., Foubert, A., Vanreusel, A., Olu-Le Roy, K., Henriët, J.-P., 2008. The distribution of scleractinian corals in the Bay of Biscay, NE Atlantic. *Facies* 54, 317–331.
- Roberts, J.M., Wheeler, A.J., Freiwald, A., 2006. Reefs of the deep: the biology and geology of cold-water coral ecosystems. *Science* 312, 543–547.
- Robinson, L.F., Belshaw, N.S., Henderson, G.M., 2004. U and Th concentrations and isotope ratios in modern carbonates and waters from the Bahamas. *Geochim. Cosmochim. Acta* 68, 1777–1789.
- Robinson, L.F., Adkins, J.F., Fernandez, D.P., Burnett, D.S., Wang, S.-L., Gagnon, A.C., Krakauer, N., 2006. Primary U distribution in scleractinian corals and its

- implications for U series dating. *Geochem. Geophys. Geosyst.* 7, Q05022. doi:10.1029/2005GC001138.
- Rogerson, M., Rohling, E.J., Weaver, P.P.E., Murray, J.W., 2004. The Azores Front since the Last Glacial Maximum. *Earth Planet. Sci. Lett.* 222, 779–789.
- Rogerson, M., Rohling, E.J., Weaver, P.P.E., Murray, J.W., 2005. Glacial to interglacial changes in the settling depth of the Mediterranean Outflow plume. *Paleoceanography* 20, PA3007. doi:10.1029/2004PA001106.
- Rüggeberg, A., Dullo, W.-C., Dorschel, B., Hebbeln, D., 2007. Environmental changes and growth history of a cold-water carbonate mound (Propeller Mound, Porcupine Seabight). *Int. J. Earth Sci.* 96, 57–72.
- Salgueiro, E., Voelker, A., Abrantes, F., Meggers, H., Pflaumann, U., Loncaric, N., González-Álvarez, R., Oliveira, P., Bartels-Jónsdóttir, H.B., Moreno, J., Wefer, G., 2008. Planktonic foraminifera from modern sediments reflect upwelling patterns off Iberia: insights from a regional transfer function. *Mar. Micropaleontol.* 66, 135–164.
- Sarnthein, M., Tetzlaff, G., Koopmann, B., Wolter, K., Pflaumann, U., 1981. Glacial and interglacial wind regimes over the eastern tropical Atlantic and Northwest Africa. *Nature* 293, 193–196.
- Schiebel, R., Waniek, J., Bork, M., Hemleben, C., 2001. Planktic foraminiferal production stimulated by chlorophyll redistribution and entrainment of nutrients. *Deep Sea Res.* 1 48, 721–740.
- Schiebel, R., Waniek, J., Zeltner, A., Alves, M., 2002. Impact of the Azores Front on the distribution of planktic foraminifera, shelled gastropods and coccolithophorids. *Deep Sea Res.* II 49, 4035–4050.
- Schmiedl, G., de Bovée, F., Buscail, R., Charrière, B., Hemleben, C., Medernach, L., Picon, P., 2000. Trophic control of benthic foraminiferal abundance and microhabitat in the bathyal Gulf of Lions, western Mediterranean Sea. *Mar. Micropaleontol.* 40, 167–188.
- Scholz, D., Mangini, A., Felis, T., 2004. U-series dating of diagenetically altered fossil reef corals. *Earth Planet. Sci. Lett.* 218, 163–178.
- Schönfeld, J., Zahn, R., 2000. Late Glacial to Holocene history of the Mediterranean Outflow. Evidence from benthic foraminiferal assemblages and stable isotopes at the Portuguese margin. *Palaeogeogr. Palaeoclimatol. Palaeoecol.* 159, 85–111.
- Schröder-Ritzrau, A., Freiwald, A., Mangini, A., 2005. U/Th-dating of deep-water corals from the eastern North Atlantic and the western Mediterranean Sea. In: Freiwald, A., Roberts, J.M. (Eds.), *Cold-water Corals and Ecosystems*. Springer, Heidelberg, pp. 691–700.
- Sierro, F.J., Flores, J.A., Baraza, J., 1999. Late glacial to recent paleoenvironmental changes in the Gulf of Cadiz and formation of sandy contourite layers. *Mar. Geol.* 155, 157–172.
- Somoza, L., Diaz-del-Rio, V., Leon, R., Ivanov, M., Fernandez-Puga, M.C., Gardner, J.M., Hernandez-Molina, F.J., Pinheiro, L.M., Rodero, J., Lobato, A., 2003. Seabed morphology and hydrocarbon seepage in the Gulf of Cádiz mud volcano area: acoustic imagery, multibeam and ultra-high resolution seismic data. *Mar. Geol.* 195, 153–176.
- Stirling, C.H., Esat, T.M., Lambeck, K., McCulloch, M.T., 1998. Timing and duration of the Last Interglacial: evidence for a restricted interval of widespread coral reef growth. *Earth Planet. Sci. Lett.* 160, 745–762.
- Stoll, H.M., Arevalos, A., Burke, A., Ziveri, P., Mortyn, G., Shimizu, N., Unger, D., 2007. Seasonal cycles in biogenic production and export in Northern Bay of Bengal sediment traps. *Deep Sea Res.* II 54, 558–580.
- Stuut, J.-B.W., Prins, M.A., Schneider, R.R., Weltje, G.J., Jansen, J.H.F., Postma, G., 2002. A 300-kyr record of aridity and wind strength in southwestern Africa: inferences from grain-size distributions of sediments on Walvis Ridge, SE Atlantic. *Mar. Geol.* 180, 221–233.
- Stuut, J.B., Zabel, M., Stuut, J.B., Zabel, M., Ratmeyer, V., Helmke, P., Schefuß, E., Lavik, G., Schneider, R.R., 2005. Provenance of present-day eolian dust collected off NW Africa: implications for deep-marine sediment studies. *J. Geophys. Res.* 110, D04202.
- Taviani, M., Bouchet, P., Metivier, B., Fontugne, M., Delibrias, G., 1991. Intermediate steps of southwards faunal shifts testified by last glacial submerged thanatocoenoses in the Atlantic Ocean. *Palaeogeogr. Palaeoclimatol. Palaeoecol.* 86, 331–338.
- Taviani, M., Remia, A., Corselli, C., Freiwald, A., Malinverno, E., Mastrototaro, F., Savini, A., Tursi, A., 2005. First geo-marine survey of living cold-water *Lophelia* reefs in the Ionian Sea (Mediterranean basin). *Facies* 50, 409–417.
- Thiel, H., Pfannkuche, O., Schriever, G., Luchte, K., Gooday, A.J., Hemleben, C., Mantoura, R.F.C., Turley, C.M., Patching, J.W., Riemann, F., 1989. Phytodetritus on the deep-sea floor in a central region of the Northeast Atlantic. *Biol. Oceanogr.* 6, 203–239.
- Thompson, W.G., Spiegelman, M.W., Goldstein, S.L., Speed, R.C., 2003. An open-system model for U-series age determinations of fossil corals. *Earth Planet. Sci. Lett.* 210, 365–381.
- Thunell, R., Reynolds, L., 1984. Sedimentation of planktonic foraminifera: seasonal changes in species flux in the Panama Basin. *Micropaleontology* 30, 243–262.
- Tyler, P.A., Harvey, R., Giles, L.A., Gage, J.D., 1992. Reproductive strategies and diet in deep-sea nuculanid protobranchs (Bivalvia: Nuculoidea) from the Rockall Trough. *Mar. Biol.* 114, 571–580.
- Tyler, B., Amaro, T., Arzola, R., Cunha, M.R., De Stigter, H., Gooday, A., Huvenne, V., Ingels, J., Kiriakoulakis, K., Lastras, G., Masson, D.G., Oliveira, A., Pattenden, A., Vanreusel, A., Van Weering, T.C.E., Vitorino, J., Witte, U., Wolff, G., 2009. Europe's Grand Canyon: Nazaré Submarine Canyon. *Oceanography* 22, 46–57.
- Voelker, A.H.L., Lebreiro, S.M., Schönfeld, J., Cacho, I., Erlenkeuser, H., Abrantes, F., 2006. Mediterranean outflow strengthening during northern hemisphere coolings: a salt source for the glacial Atlantic. *Earth Planet. Sci. Lett.* 245, 39–55.
- Waller, R.G., Tyler, P.A., 2005. The reproductive biology of two deep-water, reef-building scleractinians from the NE Atlantic Ocean. *Coral Reefs* 24, 514–522.
- Weltje, G., 1997. End-member modeling of compositional data: numerical-statistical algorithms for solving the explicit mixing problem. *Math. Geol.* 29, 503–549.
- Wheeler, A.J., Beyer, A., Freiwald, A., de Haas, H., Huvenne, V., Kozachenko, M., Olu-Le Roy, K., Opderbecke, J., 2007. Morphology and environment of cold-water coral carbonate mounds on the NW European margin. *Int. J. Earth Sci.* 96, 37–56.
- White, M., Mohn, C., de Stigter, H., Mottram, G., 2005. Deep-water coral development as a function of hydrodynamics and surface productivity around the submarine banks of the Rockall Trough, NE Atlantic. In: Freiwald, A., Roberts, J.M. (Eds.), *Cold-Water Corals and Ecosystems*. Springer, Heidelberg, pp. 503–514.
- White, M., Roberts, J.M., van Weering, T.C.E., 2007. Do bottom-intensified diurnal tidal currents shape the alignment of carbonate mounds in the NE Atlantic? *Geo-Mar. Lett.* 27, 391–397.
- Wienberg, C., Hebbeln, D., Fink, H.G., Mienis, F., Dorschel, B., Vertino, A., López Correa, M., Freiwald, A., 2009. Scleractinian cold-water corals in the Gulf of Cádiz – first clues about their spatial and temporal distribution. *Deep Sea Res.* 156, 1873–1893.
- Wilke, I., Meggers, H., Bickert, T., 2009. Depth habitats and seasonal distributions of recent planktic foraminifera in the Canary Islands region (29°N) based on oxygen isotopes. *Deep Sea Res.* I 56, 89–106.